

# (166) Dynamic Responses of Underground Structures to Incident P, SV and Rayleigh Waves

Hirokazu Takemiya Professor, Okayama University  
Haibo Wang Doctoral Candidate, Okayama University

## INTRODUCTION

Dynamic response of underground structures such as tunnels has been studied by quite a few researchers. For simple geometry and uniform elastic full space the analytical solutions are available. But for arbitrary shape structures or complex geological conditions numerical methods are imperative. Generally, as infinite medium involved, the radiation condition must be taken into account. For large scale of structures the difference of ground motions at different position should not be neglected. The structures and part of surrounding soil can be treated by Finite Element Method as it is versatile for complex finite regions. For the infinite far field other method which can treat infinite medium efficiently and accurately has to be developed.

In the presented paper, the response of tunnels to in-plane seismic waves has been investigated by combined Finite Element Method (FEM) and Source (Try Function) Method, with former applied to structures and part of soil and latter to infinite uniform far field. The influence of far field was computed as an impedance matrix based on the principle of virtual works in both discretized and continuous forms. The impedance matrix is symmetric and added to the impedance matrix of the finite domain. In the computation of far field impedance, no interpolating function is used if the interface between finite and infinite part of soil can be given analytically. Consequently, the number of nodes on the interface, which associates with mesh of FEM, has little influence on the computation effort and accuracy of the far field impedance. Satisfied and stable results can be reached for all range of frequency in practical problems. The response to real seismic wave can be worked out with the help of Fourier transformation.

## OUTLINE OF THE NUMERICAL METHOD

The model for analysis is given in Fig.1. The finite part of soil as well as the tunnels are discretized with 8-node isoparametric elements. The influence of the infinite soil at the nodes on the interface corresponding to the mesh of finite element is given in the form of impedance matrix, which will

be added on the impedance matrix of finite part, as shown in Eqn. (1).

$$\begin{bmatrix} S_{rr} & S_{ri} \\ S_{ir} & S_{ii} + S_{ii}^g \end{bmatrix} \begin{Bmatrix} u_r \\ u_i \end{Bmatrix} = \begin{Bmatrix} F_r \\ F_i \end{Bmatrix} \quad (1)$$

in which  $i$  denotes nodes on interface and  $r$  for remaining ones. The superscript  $g$  denotes the infinite soil and  $F$  is the force acting on the nodes.

The  $S_{ii}^g$  is evaluated by Try Function Method. As shown in Fig.2, we suppose the displacement and traction along the interface  $S$  are the linear combination of the Try Functions  $L_u(s)$  and  $L_t(s)$ , which are chosen as Lamb's solutions due to surface load since they satisfy both free surface and radiation condition,

$$\{u(s)\} = [L_u(s)]\{p\} \quad (2)$$

$$\{t(s)\} = [L_t(s)]\{p\} \quad (3)$$

where  $\{p\}$  are intensities of try functions as unknowns.

To combine the continuous solution with discrete one, the principle of virtual work has been used, that is the integration of the product of the displacement and traction along the interface must be equal to the sum of the products of nodal displacements and equivalent nodal forces for any possible displacement,

$$\int_s [L_u(s)]^T [L_t(s)] \{p\} ds = [U]^T \{f_b\} \quad (4)$$

Solving the  $\{p\}$  from above and substituting into Eqn.(2), further taking the discrete nodal displacements on the interface, we arrive

$$\{u_b\} = [U][E]^{-1}[U]^T \{f_b\} = [C]\{f_b\} = [S_{ii}^g]^{-1} \{f_b\} \quad (5)$$

The  $[C]$  in Eqn.(5) is the dynamic compliance, which is symmetric since  $[E]$  is.

The advantage of forming impedance by Eqn.(5) is that  $[U]$  can be got accurately and easily, and  $[E]$

can be computed without introducing interpolating functions if  $S$  can be given analytically, therefore both the accuracy and the efficiency have been improved. As no interpolating functions are used the number of nodes on interface has little influence on the computational effort.

For the case of incident wave the  $\{F_r\}$  is zero and  $\{F_i\} = [S_{ii}^g] \{u_i^g\}$ ,  $\{u_i^g\}$  are the scattered motion along the interface of canyon.

In order to compute the scattered motion, we consider the surface-traction boundary condition on  $S$ . Because it is a free surface for the canyon, the traction caused by sources must cancel with that caused by the incident wave in the free field  $\{f(s)\}$ . Since we are unable to fulfill this condition exactly, we turn to the virtual works done by both tractions, that is,

$$\int_s [L_u(s)]^T (L_f(s)\{p\} + \{f(s)\}) ds = \{0\} \quad (6)$$

Solving for  $\{p\}$  and substituting it into (2), plus the free field motion, we arrive the scattered motion due to the existence of canyon as

$$\{u^g(s)\} = \{u^f(s)\} + [L_u(s)][E]^{-1}\{B\} \quad (7)$$

where

$$\{B\} = - \int_s [L_u(s)]^T \{f(s)\} ds$$

and  $[E]$  are the same as in Eqn.(5).

Because most of part are same in integrations of  $\{B\}$  and  $[E]$ , they can be evaluated at once to save the computational effort.

With the solution of the displacements from Eqn.(1), the stresses in the tunnels can be evaluated by the ordinary method in FEM.

## NUMERICAL RESULTS

As an example of the proposed method, two parallel tunnels with circle section buried in uniform half space have been studied. The outer and inner diameters are 13.4(m) and 11.4(m) respectively. The top point is 17(m) below the free surface, and the distance between centers of tunnel is 27.8(m). The properties of soil are  $G = 2.8 \times 10^7 (N/m^2)$ ,  $\rho = 1.4 \times 10^3 (kg/m^3)$  and Poisson ratio 0.47. Those of tunnel are  $G_t = 1.382 \times 10^{10} (N/m^2)$ ,  $\rho_t = 2.5 \times 10^3 (N/m^3)$  and Poisson ratio 0.23. The

finite soil takes the shape of half circle of 40m in radius. 617 nodes with 53 on the interface are used in computation, as given in solid line in Fig.3. Stable results can be obtained up to 10.0Hz, which is about 3.5 elements or 8 nodes per wave length. Same amplitude of displacement of incident wave was assumed in the computation.

In Fig.3, it is given in dash line the real part of the response of finite field to incident SV wave of 5.0Hz and incident angle  $30^\circ$  to vertical line. Both tunnels are deformed in as the way of surrounded soil. Fig.4 shows the circumferential stresses of two tunnels at outer face, the difference in imaginary parts is quite obvious, which reflects the interaction between two tunnels, for some incident wave opposite results can be observed. Other stress components are small compared with circumferential ones. This may be due to the special Poisson ratio of the soil, the tunnels seem to suffer the radial load only.

Beside the response of tunnels, the strong response of the soil near tunnels were also founded as the frequency increases. Because the soil is almost saturate, liquefaction may occur.

In Fig.5 to Fig.6, are given the variation of stresses at certain point on tunnel with the frequency of incident waves, triangles and circles for left and right tunnel, solid and dash line for real and imaginary part respectively. The stresses increase with frequency for P and SV waves. And the position where maximum stress occur changes with frequency too, especially for SV wave, so that stresses in Fig.6 fluctuate around zero. If different properties of soil are used, the same phenomenon can be found for P wave. Usually, the SV wave arises larger stress in tunnels than P wave of same frequency. This means that the wave length of incident waves has strong influence on the response of the tunnels. For the case of incident Rayleigh, the results is given in Fig.7. Due to the surface concentration effect of Rayleigh wave, the stresses increase before 3.0Hz only. In practice, only low frequency waves exist in seismic wave.

The responses and stresses of tunnels vary with the incident direction too, especially for SV wave, in Fig.8 and Fig.9 give the variations of the maximum stress in each tunnel against the incident angle of P and SV waves, with solid line and dash line for left and right tunnel, respectively. At low frequency, the inclined waves induce larger stresses, while for high frequency the vertical incident waves induce largest stress or that close to largest stress, though the variations become complicated.

CONCLUSION

The combined FEM and Try Function Method has been used to compute the response of underground tunnels due to incident seismic waves. The far field impedance as well as the scattered motion of canyon are computed by the solutions of Lamb's problem for surface loading only. The responses of tunnels to waves of different frequency, wave type and incident angle have been studied. It is found that the stresses in tunnels increases with frequency of incident waves, provided the amplitude is kept same. The wave length has a strong influence on the stresses. The change of stresses in the tunnels with

incident direction is frequency dependent too. The stresses due to incidence of Rayleigh waves are significant at low frequency only.

REFERENCE

1. Lamb, H "On propagation of tremors over the surface of an elastic solid," *Phil. Trans. Royal. Soc. Lond.*, 1904  
2. H. Wang, H. Takemiya, Seismic Analysis of Buried Structures at Alluvium, *The Fourth East Asia-Pacific Conference on Structural Engineering & Construction*. 1993,

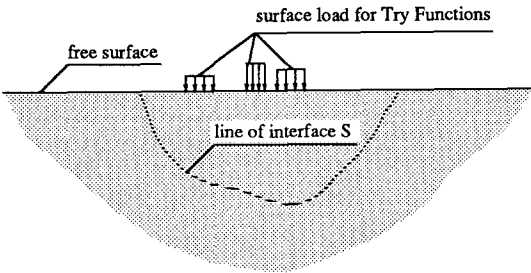
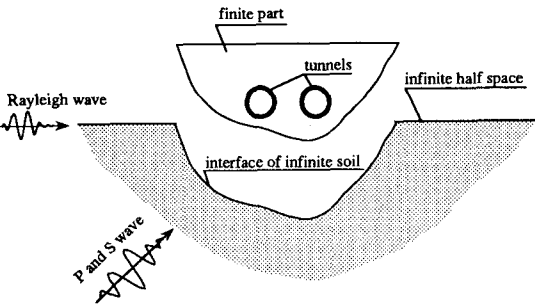


Fig.1 Model of Dynamic Soil-Structure Interaction      Fig.2 Try Function and Soil-Structure Interface

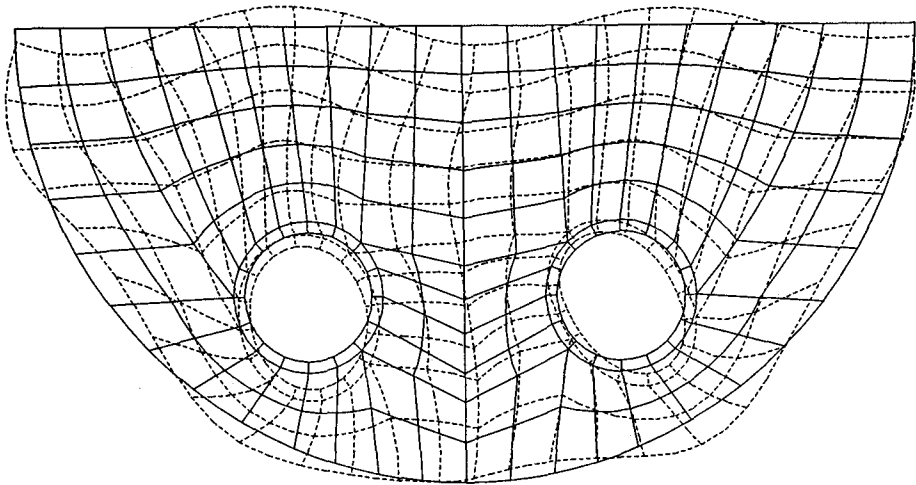


Fig.3 FEM mesh and Response of Displacement

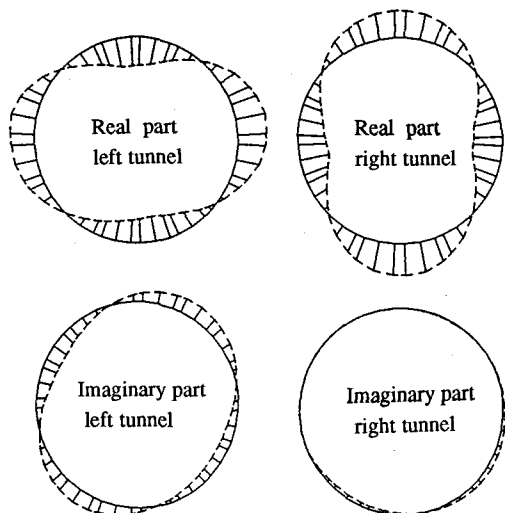


Fig.4 The Circumferential Stress in Tunnels.

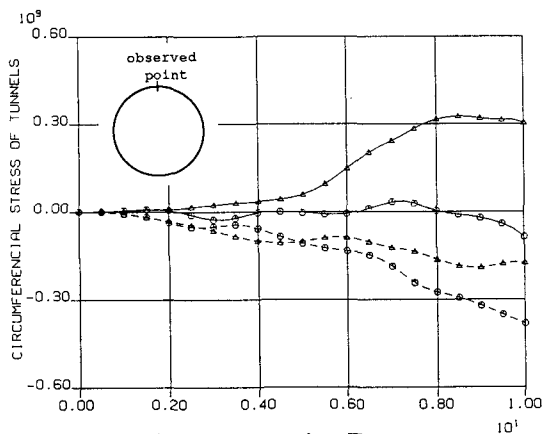


Fig.5 Stress in Tunnels against Frequency P wave incidence, angle=30° (Hz)

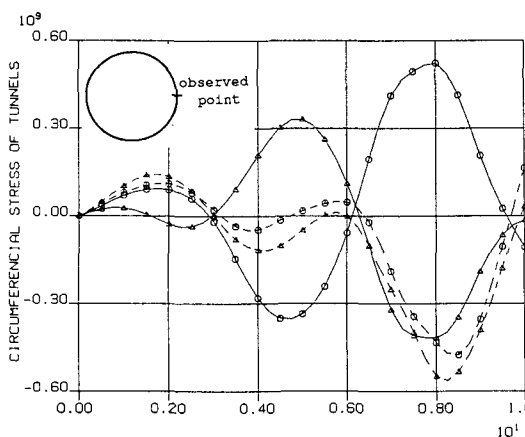


Fig.6 Stress in Tunnels against Frequency, SV wave incidence, angle=30° (Hz)

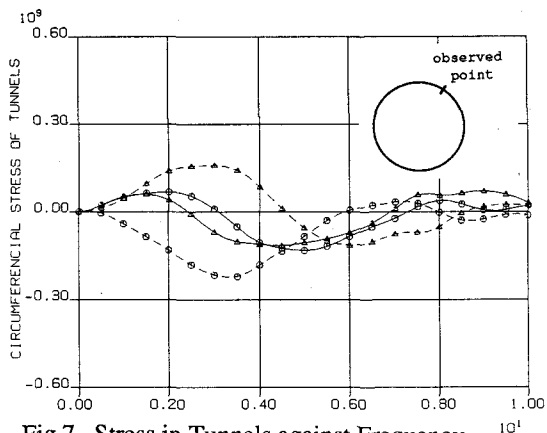


Fig.7 Stress in Tunnels against Frequency, Rayleigh wave incidence, (Hz)

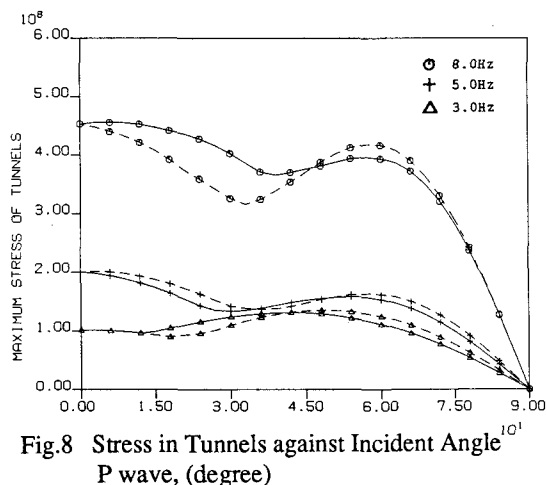


Fig.8 Stress in Tunnels against Incident Angle P wave, (degree)

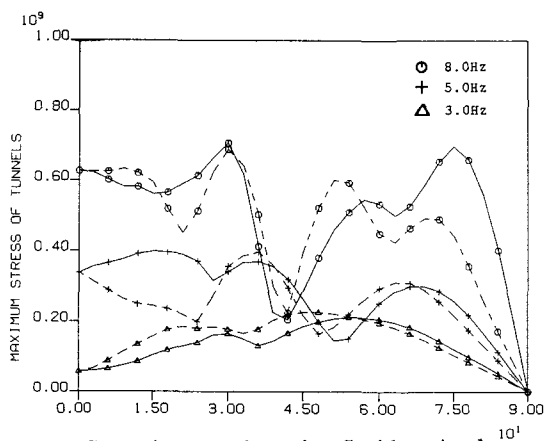


Fig.9 Stress in Tunnels against Incident Angle SV wave, (degree)